

Ultrahigh-Speed InP/InGaAs DHPTs for OEMMICs

Hideki Kamitsuna, *Member, IEEE*, Yutaka Matsuoka, *Member, IEEE*, Shoji Yamahata, *Member, IEEE*, and Naoteru Shigekawa

Abstract—This paper presents an ultrahigh-speed InP/InGaAs double-heterostructure phototransistor (DHPT) with a record optical gain cutoff frequency of 82 GHz. This excellent performance originates from the double-heterostructure's compatibility with high-performance double-heterostructure bipolar transistor (DHBT) and a new self-aligned process. To demonstrate the excellent performance of the DHPT, two kinds of optoelectronic MMICs (OEMMICs) were designed and fabricated. One is a 40-GHz-band DHPT/DHBT photoreceiver that shows the DHPT's ability to be simultaneously integrated with a high-performance DHBT. The 40-GHz operation frequency is also the highest reported for monolithically integrated HPT/HBT photoreceivers. The other is a direct optical injection-locked oscillator that can extract an electrical clock signal from optical data streams. The OEMMICs are promising for compact and low-power-consumption optical receivers on an InP platform for millimeter-wave photonics and ultrahigh-speed optical communication systems.

Index Terms—HPT, MMIC, OEIC, optical injection-locked oscillator, photoreceiver.

I. INTRODUCTION

COMPACT, high-speed, and cost-effective optical transponders that consume little power have become increasingly important for optical communication systems, including microwave photonics systems [1]. One of the most desirable pieces of hardware is an optical transceiver that consists of both optical and electronic devices on a semiconductor substrate, namely, an InP platform.

In a microwave photonics system, an optical/microwave converter is required for radio base stations. One of the most desirable configurations is to use just a photodetector plus antenna. A UTC-PD [2] combined with an optical fiber preamplifier makes it possible to eliminate an electrical postamplifier. However, a configuration of a photodetector plus an electrical amplifier without an optical preamplifier is still attractive, especially for low-cost subscriber systems. Therefore, it is still important to develop an integrated microwave/millimeter-wave photoreceiver. In an IF transmission scheme with an LO oscillator in a radio base station [3], an optoelectronic mixer is a key device. A phototransistor is one of the most promising devices for this type of application.

In multigigabit-per-second optical transmission systems, a 3R (regenerating, reshaping, and retiming) optical receiver is utilized. In this receiver, a clock recovery circuit that can extract a clock signal from transmitted data streams is a key component. The conventional fully electrical configuration usually exploits a phase-locked loop that consists of a voltage control oscillator, phase comparator, and low-pass filter. If an electrical oscillator with an optical input port, i.e., a direct optical injection-locked oscillator [4] can be applied to a clock recovery circuit, we can extremely simplify the configuration and reduce power consumption. For a direct optical injection-locked oscillator application, not only an excellent photodetection characteristic but also excellent microwave performance that can generate an oscillation is required for a phototransistor. In this application, a phototransistor is one of the most promising devices.

In both systems, ultrahigh-frequency analog circuits and/or ultrahigh-speed digital circuits are also required. Therefore, we must develop a high-performance phototransistor that is compatible with a high-performance transistor. A number of InP-based phototransistors [5]–[8] have been studied to date. Among these phototransistor structures, layer- and process-compatible heterojunction phototransistors (HPTs) based on heterojunction bipolar transistor (HBT) technology are the most promising for high-performance monolithically integrated photoreceivers [6]–[8]. Unfortunately, however, the measured and designed operation frequency of monolithically integrated HPT/HBT photoreceivers remains below 28 GHz [7], [8] and millimeter-wave (over 30 GHz) operation has never been reported to date. This is because high-speed HPTs for millimeter-wave application require both extremely high-speed base/collector photodiode operation and high maximum oscillation frequency (f_{\max}) of a transistor.

This paper presents an InP/InGaAs double-heterostructure phototransistor (DHPT) with a record optical gain cutoff frequency of 82 GHz. This performance is suitable for millimeter-wave photodetector and optically injection-locked oscillator applications. Such excellent performance comes from: 1) the elimination of low-speed holes by using the double-heterostructure; 2) high unity current gain cutoff frequency (f_T); and 3) high- f_{\max} through device size reduction by using a self-aligned process. To demonstrate the excellent performance of the DHPT, this paper also presents a 40-GHz-band optoelectronic millimeter-wave monolithic integrated circuit (OEMMIC) photoreceiver utilizing ultrahigh-speed DHPTs and double-heterostructure bipolar transistors (DHBTs). In addition, a direct optical injection-locked oscillator that can extract an electrical clock signal from optical data streams is presented.

Manuscript received December 26, 2000; revised May 18, 2001.

H. Kamitsuna and N. Shigekawa are with the NTT Photonics Laboratories, Atsugi, Kanagawa 243-0198, Japan (e-mail: kamituna@aecl.ntt.co.jp).

Y. Matsuoka was with the NTT Photonics Laboratories, Atsugi, Kanagawa 243-0198, Japan. He is now with Anritsu Corporation, Atsugi, Kanagawa 243-0855, Japan.

S. Yamahata was with NTT Photonics Laboratories, Kanagawa 243-0198, Japan. He is now with the NTT Electronics Corporation, Machida, Tokyo 194-0004, Japan.

Publisher Item Identifier S 0018-9480(01)08700-2.

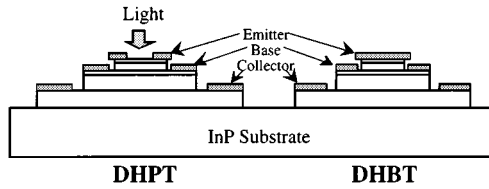


Fig. 1. Cross-sectional view of a DHPT and DHBT.

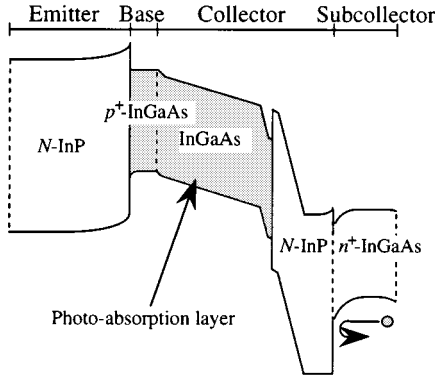


Fig. 2. Band diagram of the novel double-heterostructure for the high-speed DHPT.

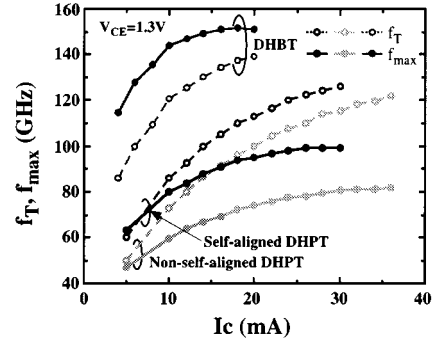
II. DEVICE STRUCTURE

Fig. 1 shows the schematic cross section of a DHPT with a simultaneously fabricated DHBT. The DHPT uses the same epitaxial layer structure for the DHBT, with a different emitter electrode pattern for optical access from the top. A 1.3- or 1.55- μm optical signal can easily penetrate into base/collector layers since most of the emitter layer consists of “transparent” InP. Since an HPT can be thought as a base/collector junction photodiode (PD-mode operation) plus an internal amplifier, such layer- and process-compatibility with the high-performance DHBT is indispensable in realizing high-performance HPT/HBT OEMMICs. For DHPT operation, this double-heterostructure, i.e., the valence band discontinuity at the interface between the N -InP collector and n^+ -InGaAs subcollector, acts as a potential barrier to low-speed holes generated in the subcollector layer as shown in Fig. 2. Therefore, we can eliminate the effect of such low-speed holes to a photoresponse, and achieve a high-speed photoresponse of the PD-mode HPT [9]. Total InGaAs layer thickness in the base/collector (photo-absorption layer) is 385 nm. Detail layer structure information is described in [7]. In addition, a self-aligned structure [10] fabricated by using the emitter electrode as a mask for emitter mesa etching is adopted to increase the high-frequency photoresponse of the DHPT through a device size reduction. This size reduction directly leads to a reduction of internal collector capacitance C_{BC} , thus reducing the CR time constant of the PD-mode DHPT. Furthermore, f_{max} , defined as

$$f_{\text{max}} \approx \sqrt{\frac{f_T}{8\pi C_{BC} R_B}}$$

can be increased. Therefore, an ultrahigh-speed DHPT with a high optical gain cutoff frequency can be obtained.

A new self-aligned DHPT, which has an optical access window (area of 20 μm^2) cut into the emitter electrode

Fig. 3. Measured f_T/f_{max} of the DHPTs and DHBT.

(emitter area of 24 μm^2) was fabricated and tested. Due to the self-aligned process, the emitter area is successfully reduced by 29.4%, while the optical access window area is exactly the same as that previously reported for a nonself-aligned DHPT [7]. For comparison, a nonself-aligned DHPT with an emitter area of 34 μm^2 and optical access window area of 20 μm^2 was also fabricated and tested.

III. DEVICE PERFORMANCE

A. Microwave Characteristics of the DHPT

Fig. 3 shows the measured f_T and f_{max} of the fabricated self-aligned DHPT and nonself-aligned DHPT, and a DHBT (emitter area of 2 $\mu\text{m} \times 10 \mu\text{m}$) at $V_{CE} = 1.3$ V. The self-aligned DHPT exhibits excellent microwave performances, i.e., high- f_T and f_{max} of 126 and 99 GHz. The f_T and f_{max} of the DHBT are 139 and 152 GHz, respectively. The layer-compatible DHPTs receive benefit from this excellent RF performance of the DHBT. Furthermore, a large increase in f_{max} of the self-aligned DHPT against that of the nonself-aligned DHPT ($f_{\text{max}} = 82$ GHz) is observed in spite of them having almost the same f_T of 122 GHz. This originates from the device size reduction. The measured f_{max} increase ratio (20.7%) agrees well with the one expected from the reduction of emitter area, which is proportional to the internal collector capacitance (C_{BC}).

Therefore, the higher f_{max} of the self-aligned DHPT comes from the device size reduction in addition to the layer-compatibility of the DHBT. Such excellent microwave performance is expected to enable millimeter-wave photodetector application.

B. Photoresponses of the DHPT

Photoresponse was measured by using a Cascade Microtech lightwave probe and an HP83467C lightwave component analyzer ($\lambda = 1.55 \mu\text{m}$). Fig. 4 shows the measured photoresponses of DHPTs under both Tr-mode ($V_{CE} = 1.3$ V, $I_C = 20$ mA) and PD-mode ($V_{CB} = 1.3$ V, $V_{BE} = 0$ V) operation. In the measurement, the base terminal was 50- Ω terminated. The vertical axis expresses $20 \log[R]$, where R is the responsivity expressed in A/W. The dc responsivity of the PD-mode for both DHPTs, including the illuminated photo-spot size mismatch, is exactly the same value, 0.25 A/W, at the optical wavelength of 1.55 μm . The higher-speed performance of the self-aligned PD-mode DHPT comes from the capacitance reduction. In addition, a high optical gain cutoff frequency of 82 GHz, the cross point between the dc responsivity of the PD-mode and the

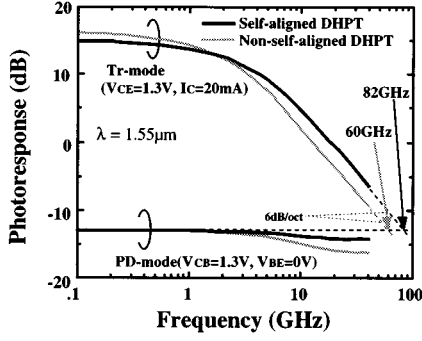


Fig. 4. Measured photoresponses of self-aligned and nonself-aligned DHPTs.

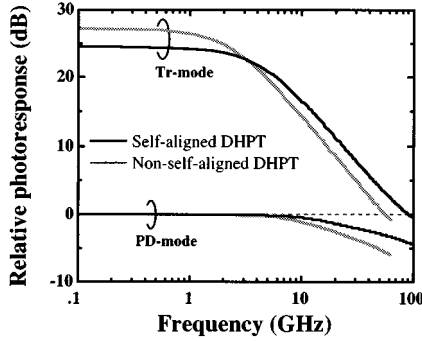


Fig. 5. Simulated relative photoresponses of self-aligned and nonself-aligned DHPTs.

extrapolation of 6 dB/oct., is achieved by the new high- f_{\max} self-aligned DHPT structure, while that of the nonself-aligned DHPT remains at 60 GHz. To our knowledge, this is the highest optical gain cutoff frequency ever reported for HPTs [8].

C. Photoresponse Simulation

To evaluate the measured photoresponse, an equivalent circuit analysis was conducted. The simulation used the equivalent circuit of the DHPT as derived from measured S -parameters under Tr- and PD-mode operation and a current source for the photo-excited carrier [7].

Fig. 5 shows the simulated relative photoresponse of the self-aligned/nonself-aligned DHPTs under both Tr- and PD-mode operation. In this figure, dc responsivity of the PD-mode is set to 0 dB. The 3-dB bandwidths are 54 and 23 GHz, respectively, for the self-aligned PD-mode DHPT and nonself-aligned PD-mode DHPT. Since these values are derived on condition that the base is 50- Ω terminated, measured results shown in Fig. 4 correspond to these simulated values. Due to the double-heterostructure shown in Fig. 2, the photoresponse for PD-mode DHPTs is limited by the CR time constant, unlike that of the conventional single-heterostructure HPT. Simulated intrinsic 3-dB bandwidths with the base terminal shorted are 76 and 43 GHz, respectively, for the self-aligned PD-mode DHPT and nonself-aligned PD-mode DHPT.

Optical gain cutoff frequencies of 90 and 56 GHz were determined for the self-aligned DHPT and nonself-aligned DHPT, respectively. These values are consistent with measured values within 10% accuracy. Therefore, we can say that the self-aligned DHPT's excellent performance originates from

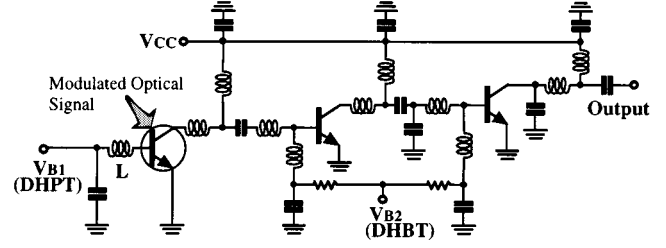


Fig. 6. Circuit diagram of the 40-GHz-band OEMMIC photoreceiver.

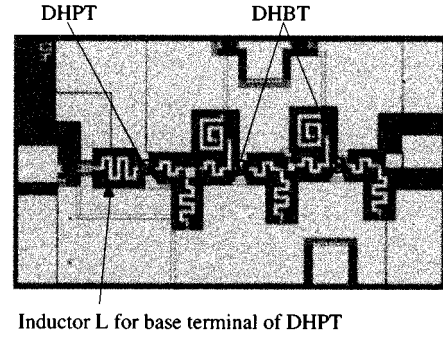


Fig. 7. Microphotograph of a DHPT/DHBT OEMMIC photoreceiver. Chip size: 1.054 mm \times 0.6 mm.

both the increase in the bandwidth of PD-mode operation and the increase in f_{\max} .

IV. OEMMIC APPLICATION

A. DHPT/DHBT Photoreceiver

To demonstrate the excellent performance of the new DHPT, which can be simultaneously integrated with a high-performance DHBT, a 40-GHz-band DHPT/DHBT OEMMIC photoreceiver was designed and fabricated. Figs. 6 and 7 show a circuit diagram and microphotograph of the fabricated DHPT/DHBT OEMMIC photoreceiver. The photoreceiver consists of a DHPT as a photodetector plus amplifier followed by reactively matched two-stage DHBT amplifier. The inductor L at the DHPT's base terminal increases the photoresponse at the 40-GHz band [7]. The design process uses the equivalent circuit models of the DHBT/DHPT, and a current source model for the O/E conversion part as was used in the discrete DHPT analysis. A π -type equivalent circuit was used for the inductor. An extremely small chip size of 1.054 mm \times 0.6 mm was achieved as a result of the lumped uniplanar MMIC structure.

Fig. 8 shows the measured photoresponse and output return loss of the DHPT/DHBT OEMMIC photoreceiver at the bias condition of $V_{CC} = 1.3$ V, $I_{DHPT} = 20$ mA, and $I_{DHBT} \times 2 = 20$ mA. The measured photoresponse of the discrete DHPT under the PD-mode is also plotted. Due to the combination of the ultrahigh-speed DHPT with the base inductor and the two-stage DHBT amplifier, the DHPT/DHBT OEMMIC photoreceiver yields a very large photodetection gain of 22 dB in comparison with the discrete PD-mode DHPT at 40 GHz. Although some MSM/HEMT OEMMIC photoreceivers that operate at millimeter-waves [11] have been reported, the 40-GHz operation frequency is the highest reported for monolithically integrated HPT/HBT photoreceivers [7], [8]. Evaluation of other important parameters

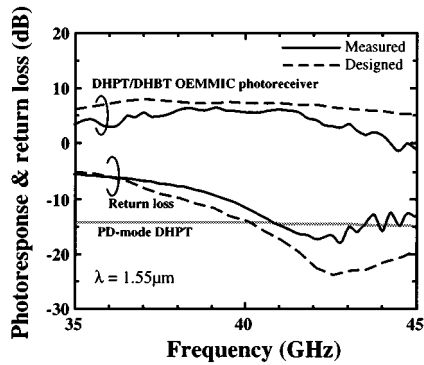


Fig. 8. Measured and designed photoresponse and return loss of the OEMMIC photoreceiver.

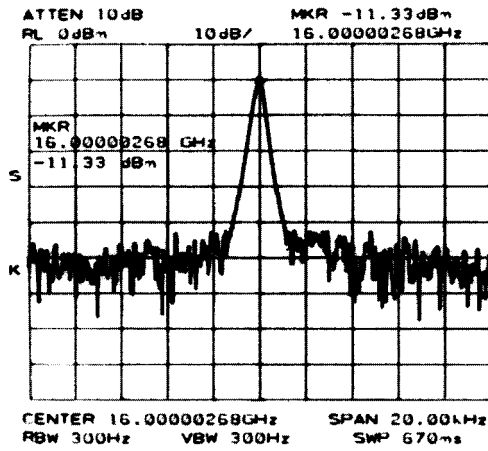


Fig. 9. Spectra of the 16-GHz-band direct optical injection-locked oscillator. Horizontal axis: 2 kHz/div. Vertical axis: 10 dB/div.

for photoreceivers, e.g., noise performance, is future work. The designed photoresponse and return loss of the OEMMIC photoreceiver are also plotted in Fig. 8. Fairly good agreement is observed between the designed and measured values for both the photoresponse and return loss.

B. DHPT Direct Optical Injection-Locked Oscillator

Five- and 16-GHz-band DHPT direct optical injection-locked oscillators were designed and fabricated as another application of a DHPT to OEMMICs. The nonself-aligned DHPTs described earlier were utilized for both oscillators. The circuit configuration is similar in [4] and based on the common-emitter series feedback configuration.

Fig. 9 shows the spectrum of an optical injection-locked oscillator for the 16-GHz band. The DHPT is illuminated directly by an optical signal with a modulation frequency of 16 GHz. The output signal is clearly locked by the modulated optical signal. To our knowledge, this is the highest reported frequency for direct optical injection locking in an InP-based HPT oscillator [12].

We tested the clock recovery ability of an oscillator for the 5-GHz band. A 4.92-Gbit/s NRZ optical signal with a 2^7-1 pseudorandom bit sequence (PRBS) is illuminated directly to the DHPT. Fig. 10 shows the experimental setup and the waveform. The upper waveform is the input signal, and the lower one is the

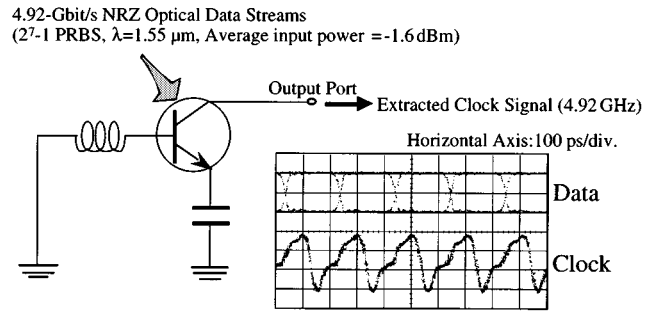


Fig. 10. Clock extraction experimental setup and input/output waveforms.

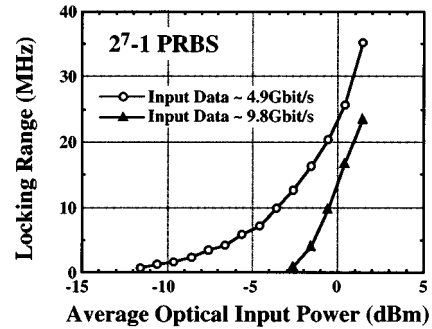


Fig. 11. Locking range characteristics for fundamental and 1/2 clock extraction from 4.9- and 9.8-Gbit/s 2^7-1 PRBS signals, respectively.

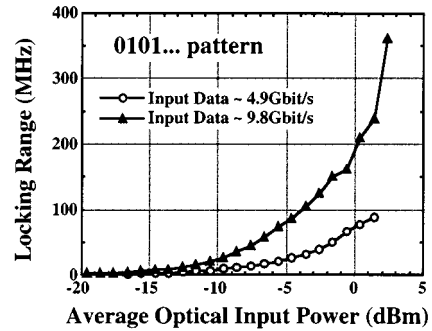


Fig. 12. Locking range characteristics for fundamental and 1/2 clock extraction from 4.9- and 9.8-Gbit/s 0101... pattern, respectively.

extracted electrical clock. It is clear that this oscillator can extract the electrical clock signal from an NRZ optical data stream by itself. Power consumption is as low as 13 mW. The oscillator makes it possible to greatly simplify the circuit configuration and lower the power consumption compared to the conventional fully electrical clock recovery circuit.

Fig. 11 shows the measured locking range characteristics of the oscillator. Fundamental and 1/2 clock extraction abilities were tested by using 4.9- and 9.8-Gbit/s 2^7-1 PRBS signals, respectively. A maximum locking range of 35 MHz was obtained for fundamental clock extraction. Fig. 12 shows locking range performances for a 0101... pattern. Since a 0101... pattern has a strong peak power at a 1/2 frequency of data rate, maximum locking range of 360 MHz was achieved for 1/2 clock extraction from 9.8-Gbit/s signals. This wide locking range corresponds to approximately a 7% relative locking range normalized to the oscillation frequency. This is sufficiently wide for practical application.

Although we used a relatively low frequency in our tests, it is possible to make a millimeter-wave oscillator with self-aligned DHPTs.

V. CONCLUSION

Owing to the double-heterostructure's compatibility with a high-performance DHBT and a new self-aligned process, we have achieved an ultrahigh-speed DHPT with a record optical gain cutoff frequency of 82 GHz. Such excellent performance originates from the ultrahigh-speed PD-mode DHPT with a 3-dB bandwidth of 76 GHz (simulated) and extremely high f_{max} of 99 GHz. A 40-GHz-band OEMMIC photoreceiver based on the DHPT/DHBT structure and DHPT direct optical injection-locked oscillators have also been presented. The DHPT and OEMMICs hold great promise as key devices for an InP platform. They should enable us to build compact, high-performance equipment for optical communication systems, including microwave photonics systems. This is because the structure of the DHPT allows us to integrate a high-frequency analog circuit with an over-10-Gbit/s digital circuit.

ACKNOWLEDGMENT

The authors thank H. Niiyama, H. Fushimi, and K. Takahata for helpful advice in measurements. They also thank Y. Ishii, H. Toba, and T. Enoki for their continuous support and encouragement.

REFERENCES

- [1] *IEEE Trans. Microwave Theory Tech. (Special Issue)*, vol. 47, July 1999.
- [2] T. Ishibashi, N. Shimizu, S. Kodama, H. Ito, T. Nagatsuma, and T. Furuta, "Uni-traveling-carrier photodiodes," in *Ultrafast Electron. Optoelectron. Tech. Dig.*, 1997, pp. 83–87.
- [3] H. Kamitsuna and H. Ogawa, "Monolithic image-rejection optoelectronic up-converters that employ the MMIC process," *IEEE Trans. Microwave Theory Tech.*, vol. 41, pp. 2323–2329, Dec. 1993.
- [4] H. Kamitsuna, "A 15-GHz direct optical injection-locked MMIC oscillator using photosensitive HBTs," *IEICE Trans. Electron.*, vol. E79-C, no. 1, pp. 40–45, Jan. 1996.
- [5] J. C. Campbell and K. Ogawa, "Heterojunction phototransistors for long-wavelength optical receivers," *J. Appl. Phys.*, vol. 53, pp. 1203–1208, Feb. 1982.
- [6] S. Chandrasekhar, L. M. Lunardi, A. H. Gnauck, R. A. Hamm, and G. J. Qua, "High-speed monolithic p-i-n/HBT and HPT/HBT photoreceivers implemented with simple phototransistor structure," *IEEE Photon. Technol. Lett.*, vol. 5, pp. 1316–1318, Nov. 1993.
- [7] H. Kamitsuna, Y. Matsuoka, S. Yamahata, and K. Kurishima, "A monolithically integrated photoreceiver realized by InP/InGaAs double-heterostructure bipolar transistor technologies for optical/microwave interaction systems," in *IEEE GaAs IC Symp. Dig.*, Oct. 1995, pp. 185–188.
- [8] C. Gonzalez, J. Thuret, J. L. Benchimol, and M. Riet, "InP/InGaAs bipolar phototransistor as a front-end photoreceiver for HFR distribution networks," in *Int. Microwave Photon. Topical Meeting Dig.*, Nov. 1999, pp. 35–38.
- [9] Y. Matsuoka and E. Sano, "InP/InGaAs double-heterostructure bipolar transistors for high-speed ICs and OEICs," *Solid-State Electron.*, vol. 38, pp. 1703–1709, Sep. 1995.
- [10] Y. Matsuoka, S. Yamahata, K. Kurishima, and H. Ito, "Ultrahigh-speed InP/InGaAs double-heterostructure bipolar transistors and analyses of their operation," *Jpn. J. Appl. Phys.*, pt. 1, vol. 35, no. 11, pp. 5646–5654, Nov. 1996.
- [11] A. Umbach *et al.*, "Technology of InP-based 1.55- μm ultrafast OEMMIC's: 40-Gbit/s broad-band and 38/60-GHz narrow-band photoreceivers," *IEEE J. Quantum Electron.*, vol. 35, pp. 1024–1031, July 1999.
- [12] P. Freeman, X. Zhang, I. Vurgaftman, J. Singh, and P. Bhattacharya, "Optical control of 14 GHz MMIC oscillators based on InAlAs/InGaAs HBT's with monolithically integrated optical waveguides," *IEEE Trans. Electron Devices*, vol. 43, pp. 373–379, Mar. 1996.



Hideki Kamitsuna (M'91) received the B.S. and M.S. degrees in physics from Kyushu University, Fukuoka, Japan, in 1986 and 1988, respectively.

In 1988, he joined the NTT Radio Communication Systems Laboratories, Yokosuka, Japan, where he was engaged in research on MMICs. In March 1990, he joined ATR Optical and Radio Communications Research Laboratories, Kyoto, Japan, on leave from NTT, where he was engaged in research on MMICs for future personal communication systems.

In March 1993, he returned to the NTT Wireless Systems Laboratories, where he was engaged in research and development on microwave photonics including monolithically integrated photoreceivers, MMICs for satellite onboard phased array systems, and MMIC power amplifiers for wireless LANs. Since August 1999, he has been with the NTT Photonics Laboratories, Atsugi, Japan, as a Senior Research Engineer. His current interests are ultrahigh-speed optical and electronic devices/ICs for optical communication systems.

Mr. Kamitsuna is a member of the Institute of Electronics, Information and Communication Engineers (IEICE), Japan. He received the 1994 Young Engineer Award presented by the IEICE. He was also a recipient of the 2000 EuMC Microwave Prize presented at the 30th European Microwave Conference, Paris, France.



Yutaka Matsuoka (M'92) received the B.S. and M.S. degrees in physics from the Tokyo Institute of Technology, Tokyo, Japan, in 1974 and 1976, respectively.

In 1976, he joined the Electrical Communication Laboratories, Nippon Telegraph and Telephone Corporation (NTT), where he has been engaged in research on electrical characterization of Si and GaAs substrates, high-speed GaAs MESFETs, GaAs- and InP-based HBTs, PDs, HPTs, ultrahigh-speed optical communication ICs/OEICs and microwave/millimeter-wave photonics. In 2000, he joined Anritsu Corporation, Kanagawa, Japan, where he is in charge of developments of HBT/IC technologies.



Shoichi Yamahata (M'92) received the B.S. and M.S. degrees in polymer science and the Ph.D. degree in physics from Hokkaido University, Hokkaido, Japan, in 1982, 1984, and 1996, respectively.

He joined the NTT Electrical Communications Laboratories, Kanagawa, Japan, in 1984, where he was involved with ion-implantations for III–V compound semiconductors. Since 1989, he has been engaged in research on GaAs- and InP-based HBTs at the NTT Photonics Laboratories, Kanagawa, Japan. His current research interests include the high-frequency characteristics of devices and their fabrication technique.

Dr. Yamahata is a member of the Japan Society of Applied Physics.



Naoteru Shigekawa received the B.S., M.S., and Ph.D. degrees in physics from the University of Tokyo, Tokyo, Japan, in 1984, 1986, and 1993, respectively.

He joined Atsugi Electrical Communications Laboratories, NTT, Kanagawa, Japan, in 1986, and was engaged in research of hot carrier transport in III–V compound-semiconductor heterostructures. From 1993 to 1994, he was a Visiting Scientist at the Department of Physics, University of Nottingham, U.K., where he worked on resonant-tunneling heterojunction bipolar transistors. Currently, he is with NTT Photonics Laboratories, Kanagawa, Japan. His current research interests are carrier transport and device physics in GaAs-, InP-, and GaN-based electron devices.

Dr. Shigekawa is a member of the Physical Society of Japan, the Japan Society of Applied Physics, the American Physical Society, and the Institute of Physics.